THE BELL SYSTEM TECHNICAL JOURNAL
Vol. 60, No. 2, February 1981
Printed in U.S.A.

Modeling Multipath Fading Responses Using Multitone Probing Signals and Polynomial Approximation

By L. J. GREENSTEIN and B. A. CZEKAJ

(Manuscript received August 7, 1980)

We show in quite a general way that highly accurate modeling of multipath fading responses is possible using low-order complex polynomials. This applies to all terrestrial radio systems in the channelized common carrier bands below 15 GHz, where channel widths are 40 MHz or less. The context of the study is a new multipath experiment being conducted in New Jersey over a 23-mile path at 11 GHz. The transmitted signal consists of up to nine tones in a 40-MHz bandwidth. These tones are coherently processed, sampled, and digitized in the receiver and recorded, during fading events, for later off-line reductions. Simple routines can be used to determine polynomial coefficients from these recorded data. This paper describes the signal processing and data reduction methods and analyzes them to assess the accuracy of polynomial fitting. The analysis uses a mean-square error measure and assumes a representative form for the underlying response function. Our results predict that the vast majority of multipath fading responses can be accurately approximated over bandwidths of 40 (62) MHz using first- (second-) order complex polynomials.

I. INTRODUCTION

Multipath fading (hereafter abbreviated MPF) on terrestrial microwave paths can be a major cause of outage in digital radio systems.[1-4] Numerous efforts have been aimed at understanding, analyzing, and correcting this source of disruption, and some have led to new statistical models for MPF responses.[5-9]

The particular model that inspires the present work approximates the MPF response by a low-order complex polynomial in frequency.[8] For a particular 26-mile path in Georgia, it was shown that a first-order polynomial suffices to characterize the fading response in a 25-

MHz band centered near 6 GHz. The joint probability distribution for the polynomial coefficients was derived for that path, thus permitting a complete statistical description of the MPF response.

Now another experiment is being instrumented, this time for a 23-mile path in New Jersey operating in the 11-GHz band. The aim of the new experiment is to add to, and in several respects improve upon, the data base used to quantify the earlier polynomial model. The improvements include higher measurement signal to noise ratios (SNRs), higher sampling rates (20 measurements per second rather than 5), coherent processing to obtain phase information (previously absent), and a wider measurement bandwidth (40 MHz rather than 25 MHz).

Given the highly variable nature of multipath fading, such improved measurements for a new path in a different frequency band and locale should add importantly to our knowledge of this phenomenon.

The basic design of the experiment can be simply stated: As many as nine coherently-phased tones within a 40-MHz bandwidth are transmitted from Murray Hill and coherently demodulated in a receiver at Crawford Hill; the demodulated tones are sampled, digitized, and screened by a desktop computer/controller; and the digitized data, if deemed interesting, are recorded on magnetic tape for later off-line processing.

The recorded data will be in a form that facilitates polynomial approximation using simple, efficient computer routines. The data will be quite general in form, however, i.e., amenable to modeling via any mathematical approximation considered promising.

The present study evaluates the accuracy of polynomial approximation, relating it to the experiment parameters and to the methods of signal processing and data reduction. Section II describes the signal processing in the transmitter and receiver, and derives signal and noise relationships used in the subsequent error analyses. Section III describes the methods of polynomial fitting to be considered, and defines the mean-square error measures that will be used to evaluate them.

Section IV analyzes the errors in the polynomial fitting caused by measurement noise, and Section V analyzes the errors caused by finite sampling of the frequency response. In general, the errors increase with the bandwidth over which the fitting is done. In analyzing the errors caused by finite sampling, we assume a general form for the MPF response function that has been applied successfully in other data-fitting studies,[5] and assume either worst-case or typical values for the function parameters.

The mean-square error calculations permit predictions of the maximum bandwidths for which polynomial fitting is valid. Section VI summarizes the results computed, under rather stringent mean-square error requirements, for polynomial orders of one, two, four, six, and eight.

II. SIGNAL PROCESSING ANALYSIS FOR THE MPF EXPERIMENT

2.1 Propagation path and radio channels

Multipath fading responses are to be measured on a 23-mile path betwen Murray Hill and Crawford Hill, similar to the one used by Crawford and Jakes in their earlier experiments.[10] The transmitting antenna at Murray Hill is 655 feet above sea level, and the receiving antenna atop Crawford Hill is 425 feet above sea level. An experimental license has been obtained to operate over this path in three 40-MHz channels within the 11-GHz common carrier band. These channels are centered at 11.465, 11.545, and 11.625 GHz. The initial measurements will be in the band centered at 11.545 GHz.

We describe here the signal processing relationships that underlie the experiment design. The details of circuitry, components, and equipment will be reported separately by those who have developed the MPF measurement system.

2.2 Transmitted signal

The transmitted signal is created by the two-stage upconversion of a baseband signal having the form

$$b(t) = d_0 + \sum_{n=1}^{N/2} d_n \cos(n\Delta\omega t + \theta_n), \tag{1}$$

where N is even and the other parameters will be discussed. The upconversion places the signal in an RF channel centered at radian frequency $\omega_c = 2\pi f_c$ ($f_c = 11.545$ GHz). Hence, the transmitted signal is

$$V_T(t) = \sum_{n=-N/2}^{N/2} \sqrt{2p_n} \cos(\omega_c t + n\Delta\omega t + \theta_n), \tag{2}$$

where p_n is the power of the nth transmitted tone and a total of $N + 1$ tones are transmitted. From (1), we see that p_0 is proportional to d_0^2 and that p_n ($n \neq 0$) bears the same proportionality to $d_n^2/4$.

The variation of p_n with n is clearly symmetrical about $n = 0$ because it derives from amplitude settings of the baseband tones. Nonuniform variations of p_n can easily be compensated for via baseband adjustments in the receiver. In Section IV we consider nonuniform variations for which receiver noise effects are minimized.

The frequency spacing between transmitted tones, Δf, may be 5, 10, or 20 MHz. Since the transmission is confined to a channel of 40-MHz width, and occupies a bandwidth $N\Delta f$, we have the constraints $(N + 1) \leq 9$ tones when $\Delta f = 5$ MHz; $(N + 1) \leq 5$ tones when $\Delta f = 10$ MHz; and $(N + 1) \leq 3$ tones when $\Delta f = 20$ MHz. We will consider the four particular combinations $N = 2$, $\Delta f = 20$ MHz; $N = 4$, $\Delta f = 10$ MHz; $N = 6$, $\Delta f = 5$ MHz; and $N = 8$, $\Delta f = 5$ MHz.

Finally, we mention that the $N/2$ baseband tones are derived from

a common 5-MHz reference, and so can be relatively phased in any manner desired. For purposes of analysis, we will assume all θ_n's to be zero here; since any phasings in the transmitter are easily undone in the receiver, no generality is lost. One criterion for choosing the actual θ_n's is minimization of the peak factor of the RF signal (2). The baseband phase adjustments that accomplish this have been derived for $N = 2$, 4, 6, and 8.[11] We will use the resulting minimized peak factors in making noise calculations later.

2.3 Response of the propagation medium

We denote the complex signal gain of the propagation medium by

$$F(\omega) = \frac{\text{Complex gain at radian frequency } \omega_c + \omega}{\text{Gain magnitude } (g_0) \text{ during nonfading}}. \tag{3}$$

The quantity g_0 can be computed from familiar radio path equations. Note that ω is measured from the center of the channel. During nonfading periods, $|F(\omega)| = 1$ throughout the channel bandwidth; during multipath fading, $F(\omega)$ varies with ω in a randomly time-varying manner.

The function $F(\omega)$ contains two phase factors of no interest to us. One is $\exp(j\phi_0)$, where ϕ_0 is the phase shift through the medium at $\omega = 0$; the other is $\exp(-j\omega t_p)$, where t_p is the nominal propagation time along the path. (For a 25-mile path, $t_p \doteq 0.13$ ms.) The investigation of multipath fading can be simplified, with no loss of information, by removing these two factors. Thus the function of interest to us is

$$H(\omega) = F(\omega) \exp[j(-\phi_0 + \omega t_p)]. \tag{4}$$

The aim of our modeling effort is to find suitable functions for approximating $H(\omega)$, and to statistically characterize the parameters of those functions.

We will see in Section 2.5 that the response function actually sampled by the measurement system is

$$G(\omega) = F(\omega)\exp\left[-j\left(\psi + \omega\frac{\theta}{\Delta\omega}\right)\right], \tag{5}$$

where ψ and θ are the (possibly) random or unknown phases of frequency references in the receiver. To obtain samples of the desired function $[H(\omega)]$ from samples of the measured function $[G(\omega)]$ will therefore require performing the operation

$$H(\omega) = G(\omega) \exp\left[\underbrace{j(\psi - \phi_0)}_{\Delta\Phi} + j\omega\underbrace{\left(t_p + \frac{\theta}{\Delta\omega}\right)}_{\Delta T}\right] \tag{6}$$

at each of the sampling frequencies [$\omega = 0, \pm\Delta\omega, \cdots, \pm (N/2)\Delta\omega$]. We will show later how to accomplish this in the data processing.

2.4 Decompositions of $F(\omega)$, $G(\omega)$, and $H(\omega)$

We demonstrate here a useful decomposition for complex response functions such as $F(\omega)$, $G(\omega)$, and $H(\omega)$. We will treat only $H(\omega)$, noting that the same mathematics and notation apply to $F(\omega)$ and $G(\omega)$.

Since ω is measured from an arbitrary microwave frequency ($2\pi f_c$), there is no physical reason to assume complex conjugate symmetry for $H(\omega)$. In its most general form, $H(\omega)$ can be expressed as

$$H(\omega) = H_a(\omega) + jH_b(\omega), \tag{7}$$

where $H_a(\omega)$ and $H_b(\omega)$ are each functions having complex conjugate symmetry. Accordingly, we can write

$$H_a(\omega) = \underbrace{H_{ar}(\omega)}_{\substack{\text{Real,}\\ \text{Even}}} + \underbrace{jH_{ai}(\omega)}_{\substack{\text{Imaginary,}\\ \text{Odd}}}, \qquad H_b(\omega) = \underbrace{H_{br}(\omega)}_{\substack{\text{Real,}\\ \text{Even}}} + \underbrace{jH_{bi}(\omega)}_{\substack{\text{Imaginary,}\\ \text{Odd}}}. \tag{8}$$

By transmitting and coherently receiving $N + 1$ tones spaced by $\Delta\omega$, one could in theory obtain measurements of the two even functions at $\omega = 0, \Delta\omega, \cdots, (N/2)\ \Delta\omega$; and of the two odd functions at $\omega = \Delta\omega, \cdots, (N/2)\ \Delta\omega$. [The total number of samples, $2(N + 1)$, is consistent with measuring the amplitudes and phases of the $N + 1$ received tones.] In reality, the receiver obtains these samples for the corresponding set of G functions, which differ from the H functions if ψ and θ are not both 0. Obtaining H samples from G samples is discussed in Section 2.6.

Another departure of the receiver outputs from the desired samples is the presence of measurement noise. We will defer the introduction of noise until Section 2.7.

2.5 Signal processing in the receiver

The receiver input at RF is

$$V_R(t) = g_0 \sum_{n=N/2}^{N/2} \sqrt{2p_n}\,|F_n| \cos(\omega_c t + n\Delta\omega t + \phi_n), \tag{9}$$

where $|F_n|$ and ϕ_n are the magnitude and phase of $F(n\Delta\omega)$; g_0 is the normal (nonfading) path gain, (3); and we have used (2) with all θ_n's assumed to be zero.

The signal goes through a two-stage down conversion which amounts to quadrature demodulation. That is, two baseband outputs are obtained which correspond to mixing $V_R(t)$ with $2\cos(\omega_c t + \psi)$ and with $-2\sin(\omega_c t + \psi)$. A nonzero value of ψ signifies that the RF and IF

references in the receiver are not in phase synchronism with those in the transmitter.

Each of the baseband signals consists of a dc component plus sinusoids at $\omega = \Delta\omega, \cdots, (N/2)\Delta\omega$. The nth sinusoid in each of these signals goes through quadrature demodulation, via the local references $\cos[n(\Delta\omega t + \theta)]$ and $-\sin[n(\Delta\omega t + \theta)]$, to produce two more dc outputs. These references are all derived from a 5-MHz source in the receiver, and nonzero θ signifies that this source is not in phase synchronism with the one in the transmitter.

Using (5) and ordinary trigonometric identities, the following statements can be proven:

(*i*) The dc outputs produced by demodulation via

$$\begin{pmatrix} 2\cos(\omega_c t + \psi) \\ -2\sin(\omega_c t + \psi) \end{pmatrix}$$

are

$$\begin{pmatrix} I_0 \\ Q_0 \end{pmatrix} \triangleq \begin{pmatrix} \sqrt{2p_0}\, g_0 G_{ar}(0) \\ \sqrt{2p_0}\, g_0 G_{br}(0) \end{pmatrix}. \tag{10}$$

(*ii*) The dc outputs produced by demodulation via

$$\begin{pmatrix} 2\cos(\omega_c t + \psi) \\ -2\sin(\omega_c t + \psi) \end{pmatrix}$$

and $\cos[n(\Delta\omega t + \theta)]$ are

$$\begin{pmatrix} (I-I)_n \\ (Q-I)_n \end{pmatrix} \triangleq \begin{pmatrix} \sqrt{2p_n} g_0 G_{ar}(n\Delta\omega) \\ \sqrt{2p_n} g_0 G_{br}(n\Delta\omega) \end{pmatrix}, \qquad n = 1, N/2. \tag{11}$$

(*iii*) The dc outputs produced by demodulation via

$$\begin{pmatrix} 2\cos(\omega_c t + \psi) \\ -2\sin(\omega_c + \psi) \end{pmatrix}$$

and $-\sin[n(\Delta\omega t + \theta)]$ are

$$\begin{pmatrix} (I-Q)_n \\ (Q-Q)_n \end{pmatrix} \triangleq \begin{pmatrix} \sqrt{2p_n} g_0 G_{ai}(n\Delta\omega) \\ \sqrt{2p_n} g_0 G_{bi}(n\Delta\omega) \end{pmatrix}, \qquad n = 1, N/2. \tag{12}$$

Thus, the dc outputs of the receiver correspond to evenly-spaced frequency samples of the four G functions $G_{ar}(\omega)$, $G_{ai}(\omega)$, $G_{br}(\omega)$, and $G_{bi}(\omega)$. Each of the $2(N+1)$ dc components is low-pass filtered, with a noise bandwidth of 100 Hz; time-sampled 20 times per second and quantized with 14-bit precision by a Datel System 256 acquisition system;* and passed to a HP 9845A computer for real-time screening.†

* Datel Corporation.
† Hewlett-Packard.

Any set of samples that seems interesting, or is part of a sequence that seems interesting, is recorded on magnetic tape for subsequent off-line processing.

2.6 Relating the G and H functions

By using (6), the H functions ($H_{ar}(\omega)$, $H_{ai}(\omega)$, etc.) can be easily obtained from the corresponding G functions once $\Delta\Phi$ and ΔT are specified. Defining a new function $G(\omega; \Delta\Phi) \triangleq G(\omega) \exp(j\Delta\Phi)$, we first perform the matrix operation

$$\begin{bmatrix} G_{ar}(\omega; \Delta\Phi) \\ G_{br}(\omega; \Delta\Phi) \end{bmatrix} = \begin{bmatrix} \cos \Delta\Phi & -\sin \Delta\Phi \\ \sin \Delta\Phi & \cos \Delta\Phi \end{bmatrix} \begin{bmatrix} G_{ar}(\omega) \\ G_{br}(\omega) \end{bmatrix}. \tag{13}$$

An identical equation relates $G_{ai}(\omega; \Delta\Phi)$ and $G_{bi}(\omega; \Delta\Phi)$ to $G_{ai}(\omega)$ and $G_{bi}(\omega)$. The H functions are then obtained from these new G functions, for specified ΔT, as follows:

$$\begin{bmatrix} H_{ar}(\omega) \\ H_{ai}(\omega) \end{bmatrix} = \begin{bmatrix} \cos \omega\Delta T & -\sin \omega\Delta T \\ \sin \omega\Delta T & \cos \omega\Delta T \end{bmatrix} \begin{bmatrix} G_{ar}(\omega; \Delta\Phi) \\ G_{ai}(\omega; \Delta\Phi) \end{bmatrix}. \tag{14}$$

An identical equation relates $H_{br}(\omega)$ and $H_{bi}(\omega)$ to $G_{br}(\omega; \Delta\Phi)$ and $G_{bi}(\omega; \Delta\Phi)$.

The operation indicated by (13) leads to the result $H_{br}(0) = 0$, i.e., the phase response of the function to be analyzed is forced to zero at $\omega = 0$. [To see this, combine (6), (12) and (13) for $\omega = 0$.] This is a welcome simplification in the data and entails no loss of useful information. Fortunately, $\sin \Delta\Phi$ and $\cos \Delta\Phi$ are readily obtained from the measured G samples, for

$$\sin \Delta\Phi = -\frac{G_{br}(0)}{\sqrt{G_{ar}^2(0) + G_{br}^2(0)}}, \qquad \cos \Delta\Phi = \frac{G_{ar}(0)}{\sqrt{G_{ar}^2(0) + G_{br}^2(0)}}. \tag{15}$$

To see this, use (5) at $\omega = 0$ and recall that $\Delta\Phi = \psi - \phi_0$.]

By way of contrast, the value of ΔT to use in (14) is not so readily specified or determined. Yet, to get the full benefit of polynomial modeling (i.e., accurate fitting using low-order functions), ΔT must be carefully chosen.* We have arrived at a criterion for choosing ΔT based upon the following data reduction procedure: For a given ΔT, (14) is applied and the resulting H samples are fitted by a finite-order complex polynomial in $j\omega$. We consider that value of ΔT to be optimal for which the polynomial fitting is best, in some least-squares sense

* To see why, consider the example $G(\omega) = \exp(-j\omega t_0)$, where $t_0 \approx 1/B$, and B is the bandwidth over which $H(\omega) = G(\omega) \exp(j\omega\Delta T)$ is to be fitted. If $\Delta T = 0$, $H(\omega) = \cos \omega t_0 - j \sin \omega t_0$, and high-order polynomials are needed for accurate fitting over the bandwidth. If $\Delta T = t_0$, however, $H(\omega) = 1 + j0$, and low-order polynomials are quite sufficient.

defined later. In Section 5.4, we will identify a data-derived measure that accurately predicts the optimal ΔT.

2.7 Measurement noise

We have shown that the dc receiver outputs are proportional to frequency samples of the function $G(\omega)$, and that the unwanted phase factors that distinguish $G(\omega)$ from $H(\omega)$ can be removed in the data processing. Not so readily removed are the noises associated with the digitized outputs. These consist of both additive Gaussian noise from the input and components of the receiver and quantizing noise from the 14-bit analog-to-digital conversions.

Receiver noise produces an additive random component for each dc output defined by (10) to (12). These $2(N + 1)$ noises are zero-mean and mutually independent. All have the same variance except those associated with (10), i.e., $n = 0$, for which the variance is 3 dB higher. These findings follow from the receiver processing described in Section 2.5.

We shall now assume that each of the dc outputs in (10) to (12) is adjusted by a factor $1/(g_0\sqrt{2p_n})$, $n = 0, N/2$, before being digitized. Accordingly, the variance of the Gaussian noise associated with a given output sample is

$$\sigma_G^2 = \begin{cases} kTbN_F/p_0g_0^2, & n = 0, \\ kTbN_F/2p_ng_0^2, & n = 1, N/2. \end{cases} \tag{16}$$

Table I defines the quantities in (16) and gives values for each. Using those data and assuming uniform tone powers, we obtain the following

Table I—System parameters used in noise analysis

	Parameter Definition and Assumed Value(s)
g_o^2	Power gain between transmitter output and first receiver amplifier stage; includes clear-air path loss and circuit and waveguide losses: $10 \log g_o^2 = -74$ dB
kT	Thermal noise density at receiver input: $10 \log kT = -174$ dBm/Hz
b	Noise bandwidth of receiver processing for each tone: $b = 100$ Hz
N_F	Noise figure of first receiver amplifier stage: $10 \log N_F = 2$ dB
P_p	Peak transmitter power, constrained to meet out-of-band emission requirements: $10 \log P_p = 14$ dBm
P_F	Transmitter peak factor, minimized via phase adjustments of the baseband tones before upconversion. For uniform tone powers, $10 \log P_F = \begin{cases} 7.8 \text{ dB}, & N = 2, \\ 6.3 \text{ dB}, & N = 4, \\ 6.3 \text{ dB}, & N = 6, \\ 6.6 \text{ dB}, & N = 8 \end{cases}$
$\bar{P}$	Average transmitter power: $\bar{P} = P_p/P_F$. For $N = 8$, $10 \log \bar{P} = 7.4$ dBm
p_n	Averge power in transmitted tone at frequency $\pm n\Delta\omega$ from center. For uniform tone powers and $N = 8$, $10 \log p_n = -1.8$ dBm

result: σ_G^2 in dB, for $n \neq 0$, lies in the range -79 dB $\pm$ 2 dB, where the precise value depends on N; for $n = 0$, σ_G^2 is 3 dB higher.

Assuming the dc outputs are amplitude-adjusted as indicated, the input to every 14-bit A/D conversion is precisely a sample of a G-function. During normal propagation, the G samples lie within $\pm$ 1 [see (3) and (5)]. To provide some room for excess gain, we assume quantizer amplitude limits set at $\pm$ 1.60 (4-dB margin). As a result, the quantizing error for each digitized sample can be characterized as an additive noise uniformly distributed on $[-\Delta/2, \Delta/2]$, where $\Delta = 2 \times 1.6 \times 2^{-14} = 1.95 \times 10^{-4}$. The quantizing noise variance is then

$$\sigma_Q^2 = \Delta^2/12 = 3.18 \times 10^{-9}(-85dB), \quad \text{every sample.} \tag{17}$$

Comparing this with σ_G^2 above, we find justification for ignoring quantization effects. Alternately, they can be accounted for using an approximate correction factor given in Section IV.

To simplify matters further, we introduce the notation

$$H_{ar,n} \triangleq H_{ar}(n\Delta\omega), \qquad H_{br,n} \triangleq H_{br}(n\Delta\omega), \qquad \text{etc.} \tag{18}$$

These are the quantities produced by (13) and (14) for any specified combination of $\Delta\Phi$ and ΔT. We account for the noisiness of the H samples via the notation

$$\hat{H}_{ar,n} \triangleq H_{ar,n} + \zeta_{ar,n}, \qquad \hat{H}_{br,n} \triangleq H_{br,n} + \zeta_{br,n}, \qquad \text{etc.,} \tag{19}$$

where $\zeta_{ar,n}$, $\zeta_{br,n}$, etc., are the random noise samples. Since the ζs are produced by phase rotations of the noises associated with the G samples, they are all Gaussian, zero-mean, and mutually independent, just like the original noises. Moreover, their variances are identical to σ_G^2, as given by (16). We thus have an accurate, simple description for the noisiness of the data to be processed.

III. POLYNOMIAL FITTING AND ERROR MEASURES

3.1 Fitting polynomials to the $\hat{H}$ samples

The implicit assumption of the polynomial fitting approach is that, over some finite bandwidth B centered on $f = 0$, the response function $H(\omega)$ can be accurately approximated by a low-order complex polynomial, i.e.,

$$H(\omega) \cong \hat{H}(\omega) \triangleq \sum_{k=0}^{M} (A_k + jB_k)(j\omega)^k, \qquad |\omega| \leq \pi B. \tag{20}$$

Using (7) and (8), we can break this representation down as follows:

$$H_a(\omega) \cong \sum_{k=0}^{M} A_k(j\omega)^k = \underbrace{\sum_{\substack{k=0 \\ \text{Even}}}^{M} A_k(j\omega)^k}_{\text{Fit to } H_{ar}(\omega)} + \underbrace{\sum_{\substack{k=1 \\ \text{Odd}}}^{M} A_k(j\omega)^k}_{\text{Fit to } jH_{ai}(\omega)}, \tag{21}$$

$$H_b(\omega) \cong \sum_{k=0}^{M} B_k(j\omega)^k = \underbrace{\sum_{\substack{k=0 \\ \text{Even}}}^{M} B_k(j\omega)^k}_{\text{Fit to } H_{br}(\omega)} + \underbrace{\sum_{\substack{k=1 \\ \text{Odd}}}^{M} B_k(j\omega)^k}_{\text{Fit to } jH_{bi}(\omega)}. \tag{22}$$

The A_k's and B_k's are slowly varying random coefficients; in any given measurement interval, they collectively characterize the short-term frequency response of the propagation medium.

The fittings indicated above can be done, for every 50-ms measurement interval, by using the $2(N + 1)$ $\hat{H}$ samples obtained in that interval. The way the fitting is done depends on the values of M and N. We now consider three possible cases.

Case 1: M = N, with N = 2, 4, 6, or 8

The $\hat{H}$ samples obtained using $N + 1$ tones can be fitted precisely using an Nth-order complex polynomial. Thus, when $M = N$, fitting consists of matching each summation in (21) and (22) to the appropriate $\hat{H}$ samples at the sample frequencies. The resulting equations for the A_k's are as follows (identical equations apply to the B_k's, with $\hat{H}_{br}$'s and $\hat{H}_{bi}$'s replacing the $\hat{H}_{ar}$'s and $\hat{H}_{ai}$'s):

$$A_k = \begin{cases} \hat{H}_{ar,0}, & k = 0, \\ \dfrac{1}{(\Delta\omega)^k} \displaystyle\sum_{n=1}^{N/2} D^e_{k/2,n}[\hat{H}_{ar,n} - \hat{H}_{ar,0}], & k = 2, 4, \cdots, N, \\ \dfrac{1}{(\Delta\omega)^k} \displaystyle\sum_{n=1}^{N/2} D^o_{(k+1)/2,n}\, \hat{H}_{ai,n}, & k = 1, 3, \cdots, N-1, \end{cases} \tag{23}$$

where $D^e_{l,m}$ and $D^o_{l,m}$ are the (l, m)th elements of the $N/2 \times N/2$ matrices $[D^e]$ and $[D^o]$, respectively; $[D^e]$ and $[D^o]$ are the inverses of the matrices $[d^e]$ and $[d^o]$, respectively; and the (m, l)th elements of $[d^e]$ and $[d^o]$ are

$$d^e_{m,l} = (-1)^l m^{2l} \tag{24}$$

and

$$d^o_{m,l} = -(-1)^l m^{2l-1}. \tag{25}$$

The matrices $[D^e]$ and $[D^o]$ for $N = 2$, 4, 6, and 8 are given in Table II. Note for future reference that the derived A_k's and B_k's are weighted sums of the $\hat{H}$ samples.

Since N can be as high as eight, this method of fitting suggests the possibility of eighth-order polynomial modeling. Earlier studies, however, suggest that this order is unnecessarily high for bandwidths of 20 to 40 MHz.[8,12] Reductions using $M = N = 8$ may therefore involve excessive demands on data storage and analysis, and unduly complicate

Table II—Matrices for evaluating eq. (23)

N	Matrix $[D^e]$	Matrix $[D^o]$
2	[1]	[1]
4	$-\frac{4}{3}$ $\frac{1}{12}$ $-\frac{1}{3}$ $\frac{1}{12}$	$\frac{4}{3}$ $-\frac{1}{6}$ $\frac{1}{3}$ $-\frac{1}{6}$
6	$-\frac{3}{2}$ $\frac{3}{20}$ $-\frac{1}{90}$ $-\frac{13}{24}$ $\frac{1}{6}$ $-\frac{1}{72}$ $-\frac{1}{24}$ $\frac{1}{60}$ $-\frac{1}{360}$	$\frac{3}{2}$ $-\frac{3}{10}$ $\frac{1}{30}$ $\frac{13}{24}$ $-\frac{1}{3}$ $\frac{1}{24}$ $\frac{1}{24}$ $-\frac{1}{30}$ $\frac{1}{120}$
8	$-\frac{8}{5}$ $\frac{1}{5}$ $-\frac{8}{315}$ $\frac{1}{560}$ $-\frac{61}{90}$ $\frac{169}{720}$ $-\frac{1}{30}$ $\frac{7}{2880}$ $-\frac{29}{360}$ $\frac{13}{360}$ $-\frac{1}{120}$ $\frac{1}{1440}$ $-\frac{1}{360}$ $\frac{1}{720}$ $-\frac{1}{2520}$ $\frac{1}{20160}$	$\frac{8}{5}$ $-\frac{2}{5}$ $\frac{8}{105}$ $-\frac{1}{140}$ $\frac{61}{90}$ $-\frac{169}{360}$ $\frac{1}{10}$ $-\frac{7}{720}$ $\frac{29}{360}$ $-\frac{13}{180}$ $\frac{1}{40}$ $-\frac{1}{360}$ $\frac{1}{360}$ $-\frac{1}{360}$ $\frac{1}{840}$ $-\frac{1}{5040}$

model development and usage. For this reason, we also consider the combinations $M = N = 6$, $\Delta f = 5$ MHz; $M = N = 4$, $\Delta f = 10$ MHz; and $M = N = 2$, $\Delta f = 20$ MHz.

Case 2: M = 2, with N = 8

Another possibility is to assume a low-order polynomial while using all nine tones, in which event the fittings indicated in (21) and (22) are done by least-squares methods. Compared with the case $M = N = 2$, this approach requires more data storage and analysis. On the other hand, it leads to better fitting accuracy and protects against loss of tones caused by equipment problems. Noise effects can be slightly worse for this case, despite the noise-averaging it affords, because the power per tone must be lower to satisfy the transmitter power constraint.

The least-squares polynomial fitting method is well known,[13] and so we give only the results:

$$A_0 = \frac{59}{231}\left[\hat{H}_{ar,0} + 2\sum_{n=1}^{4}\left(1 - \frac{5n^2}{59}\right)\hat{H}_{ar,n}\right], \tag{26}$$

$$A_1 = \frac{1}{30\Delta\omega}\sum_{n=1}^{4} n\hat{H}_{ai,n}, \tag{27}$$

$$A_2 = \frac{5}{231\Delta\omega^2}\left[\hat{H}_{ar,0} + 2\sum_{n=1}^{4}\left(1 - \frac{3n^2}{20}\right)\hat{H}_{ar,n}\right]. \tag{28}$$

The equations for B_0, B_1, and B_2 are identical, with $\hat{H}_{br,n}$ and $\hat{H}_{bi,n}$ replacing $\hat{H}_{ar,n}$ and $\hat{H}_{ai,n}$. Again, the A_k's and B_k's are weighted sums of the $\hat{H}$ samples.

Case 3: M = 1, with N = 8

The case $M = 1$ represents the ultimate in modeling simplicity, namely, a response function which is first order in $j\omega$. Strong experimental evidence for such a polynomial has been reported.[8,9] Assuming least-squares fitting to nine tones, we find that

$$A_0 = \frac{1}{9}\left[\hat{H}_{ar,0} + 2\sum_{n=1}^{4}\hat{H}_{ar,n}\right]; \tag{29}$$

A_1 is given by (27); and the same equations give B_0 and B_1, with $\hat{H}_{br,n}$ and $\hat{H}_{bi,n}$ replacing $\hat{H}_{ar,n}$ and $\hat{H}_{ai,n}$.

3.2 Error measures

The MPF response function, as reconstructed from the data-derived A_k's and B_k's, is

$$\hat{H}(\omega) = \sum_{k=0}^{M}(A_k + jB_k)(j\omega)^k. \tag{30}$$

Since the coefficients are weighted sums of noisy H samples, (19), we can write $\hat{H}(\omega)$ in the form

$$\hat{H}(\omega) = \underset{\substack{\text{Weighted sum}\\ \text{of true}\\ H \text{ samples}}}{\tilde{H}(\omega)} + \underset{\substack{\text{Weighted sum}\\ \text{of random}\\ \text{noise samples}}}{Z(\omega)} \tag{31}$$

Whereas $\tilde{H}(\omega)$ is noiseless, it is not identical to the true response function, $H(\omega)$, but is a polynomial approximation.

We now define the error function

$$\begin{aligned}\epsilon(\omega) &\triangleq \hat{H}(\omega) - H(\omega)\\ &= \underset{\substack{\text{Approximation}\\ \text{error, } \epsilon(\text{approx})}}{[\tilde{H}(\omega) - H(\omega)]} + \underset{\substack{\text{Noise error,}\\ \epsilon(\text{noise})}}{Z(\omega)}\end{aligned} \tag{32}$$

If B is some bandwidth about f_c over which $H(\omega)$ is to be characterized, then the mean-square error for a given polynomial fit can be defined as

$$\begin{aligned}\overline{\epsilon^2} &\triangleq \frac{1}{B}\int_{-B/2}^{B/2}|\epsilon(\omega)|^2\,df\\ &= \underbrace{\frac{1}{B}\int_{-B/2}^{B/2}|\tilde{H}(\omega) - H(\omega)|^2\,df}_{\overline{\epsilon^2(\text{approx})}} + \underbrace{\frac{1}{B}\int_{-B/2}^{B/2}|Z(\omega)|^2\,df}_{\overline{\epsilon^2(\text{noise})}}.\end{aligned} \tag{33}$$

A useful normalizing quantity for these mean-square errors is the mean-square gain of the fading channel, i.e.,

$$\overline{H^2} \triangleq \frac{1}{B}\int_{-B/2}^{B/2} |H(\omega)|^2\, df. \tag{34}$$

Radio system experience has shown that, for $B \geq 20$ MHz, $\overline{H^2}$ is seldom lower than 10^{-4} (40-dB total power fade).

Let us now interpret B as the bandwidth over which the intended receiver output (undistorted by MPF) has a roughly uniform power spectrum, and outside which the spectral content is small. Accordingly, $\overline{\epsilon^2}$ accurately represents the mean-square error in predicting the output signal using $\hat{H}(\omega)$ for the MPF response and $\overline{H^2}$ accurately represents the true mean-square output. It is thus reasonable to say that a given polynomial fit is valid if $\overline{\epsilon^2(\text{noise})}/\overline{H^2}$ and $\overline{\epsilon^2(\text{approx})}/\overline{H^2}$ are both 10^{-3} or less. Since $\overline{\epsilon^2(\text{noise})}$ is independent of $H(\omega)$, and since $\overline{H^2}$ is seldom lower than 10^{-4}, our requirement for $\overline{\epsilon^2(\text{noise})}$ is that it be 10^{-7} or less.

IV. MEASUREMENT NOISE ERRORS

4.1 Method of analysis

We compute $\overline{\epsilon^2(\text{noise})}$ by forming $Z(\omega)$ in (31), using (30) and the governing formulas for A_k and B_k. For simplicity, we use the first-order model (Case 3: $M = 1$, $N = 8$) to exemplify the approach.

From (30) and (31),

$$Z(\omega) = \sum_{k=0}^{1} (\delta A_k + j\delta B_k)(j\omega)^k, \tag{35}$$

where δA_0 and δA_1 are the noises in A_0 and A_1, which are computed using (27) and (29); and similar definitions and equations apply for δB_0 and δB_1. There noises are related to the noise components $\zeta_{ar,0}$, $\zeta_{ar,1}$, etc., in the $\hat{H}$ samples of (27) and (29). Thus,

$$\delta A_0 = \frac{1}{9}\left[\zeta_{ar,0} + 2\sum_{n=1}^{4}\zeta_{ar,n}\right], \qquad \delta A_1 = \frac{1}{30\Delta\omega}\sum_{n=1}^{4} n\zeta_{ai,n}, \tag{36}$$

and similarly for δB_0 and δB_1. We now proceed in the obvious way: δA_0, δA_1, etc., are combined with (35); $|Z(\omega)|^2$ is formed; and the integration in (33) is performed to obtain $\overline{\epsilon^2(\text{noise})}$. In doing so, we make use of the statistical independence among all the noise samples. We also use (16) for their variances. The result is of the form

$$\overline{\epsilon^2(\text{noise})} = \frac{kTbN_F}{2g_0^2}\sum_{n=0}^{N/2}\frac{S_n(B/\Delta f)}{p_n}, \tag{37}$$

where, for the case under study, $N = 8$ and

$$S_n(B/\Delta f) = \frac{4}{81}\left[1 + \frac{3}{1600}\left(\frac{B}{\Delta f}\right)^2 n^2\right], \qquad n = 0, N/2. \tag{38}$$

For all of the other cases considered, the analytical approach and the form of the result are as shown above; only the specific equations for $S_n(B/\Delta f)$ vary.

The final step in computing $\overline{\epsilon^2(\text{noise})}$ is to specify the values of the transmitted tone powers. We have considered two approaches, namely (*i*) assuming all p_n's to be equal, adding up to some specified value ($\bar{P}$) of average transmitted power; and (*ii*) choosing the p_n's so as to minimize $\overline{\epsilon^2(\text{noise})}$, subject to the same average power specification. In the first approach, we apportion power according to the rule

$$p_n = \frac{\bar{P}}{N+1}, \quad \text{all } n. \tag{39}$$

In the second approach, we use the method of Lagrangian multipliers to minimize (37), subject to the constraint

$$p_0 + 2\sum_{n=1}^{N/2} p_n = \bar{P}. \tag{40}$$

The result in that case is

$$p_n = \frac{\sqrt{(1+\delta_n^0)S_n(B/\Delta f)}\,\bar{P}}{\sqrt{2S_0(B/\Delta f)} + 2\sum_{n=1}^{N/2}\sqrt{S_n(B/\Delta f)}}, \quad \text{all } n, \tag{41}$$

where δ_n^0 is the Kronecker delta function. Note that the optimal variation of p_n with n depends on the bandwidth ratio, $B/\Delta f$.

We have reduced (37) to numerical results using the parameter values in Table I. We now present our findings.

4.2 Results for Case 1 ($M = N = 2, 4, 6,$ or 8)

Figure 1 shows curves of $\overline{\epsilon^2(\text{noise})}$ vs. B for the various possibilities under Case 1. We can make the following observations:

(*i*) The noise errors and their rate-of-growth with B depend strongly on the polynomial order M, both being less for lower M. From a noise standpoint then, M should be chosen to be low. The competing factor influencing this choice is the approximation error, which we consider later.

(*ii*) Optimizing p_n does not improve significantly on the use of uniform tone powers. There is no compelling reason, therefore, to taper the p_n's. On the other hand, doing so entails no price in complexity and may offer benefits, e.g., tapering of p_n may reduce out-of-band spurious tones caused by transmitter nonlinearities. We will not explore this topic here, but present in Table III some examples of optimal p_n variations.

(*iii*) Values of $\overline{\epsilon^2(\text{noise})}$ less than 10^{-7} can be attained, using either uniform or optimal p_n's, for bandwidths up to 34 MHz or more, depending on M. For purposes of modeling, errors of this magnitude can be regarded as negligible, as noted in Section 3.2.

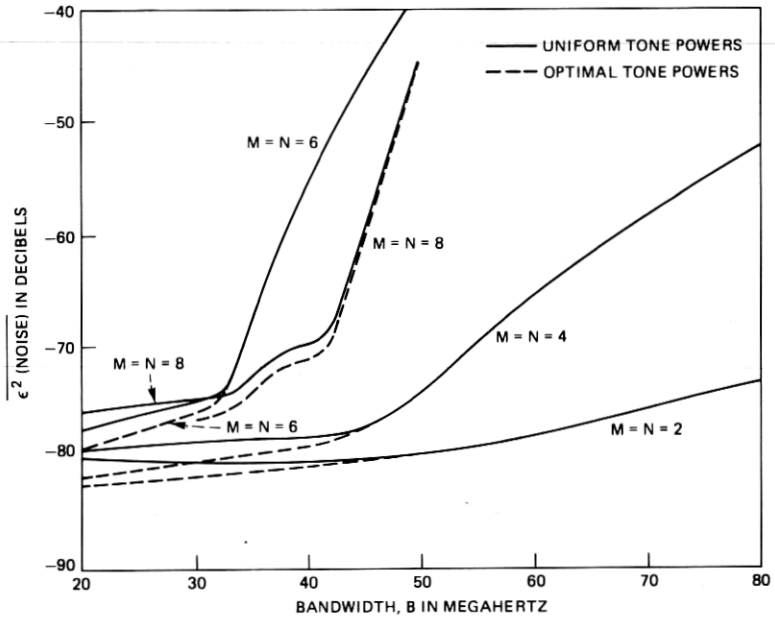

Fig. 1—Mean-square noise errors, $\overline{\epsilon^2(\text{noise})}$ in dB, for Case 1 ($M = N = 2$, 4, 6 or 8). For each N, the curve for optimal tone powers (dotted) merges with the one for uniform tone powers (solid).

4.3 Results for Cases 2 and 3 ($M = 2$, $N = 8$ and $M = 1$, $N = 8$)

Figure 2 shows curves of $\overline{\epsilon^2(\text{noise})}$ vs. B for Cases 2 and 3. These results show the effects of noise when first- and second-order polynomials are formed via least-squares fitting to nine received tones. For purposes of comparison, Fig. 2 also repeats the results for $M = N = 2$ under Case 1, i.e., second-order matching to three received tones. We note the following:

(i) As before, fitting $H(\omega)$ with a lower-order polynomial leads to smaller noise-related errors.

(ii) Comparing the two ways of getting $M = 2$, noise errors are

Table III—Optimal tone powers for Case 1, B = 40 MHz (in dB above power of central tone)

Frequency / N	±5 MHz	±10 MHz	±15 MHz	±20 MHz
2	—	—	—	−3.02
4	—	−0.10	—	−4.05
6	−0.80	−3.30	−7.60	—
8	−0.36	−1.36	−2.63	−7.95

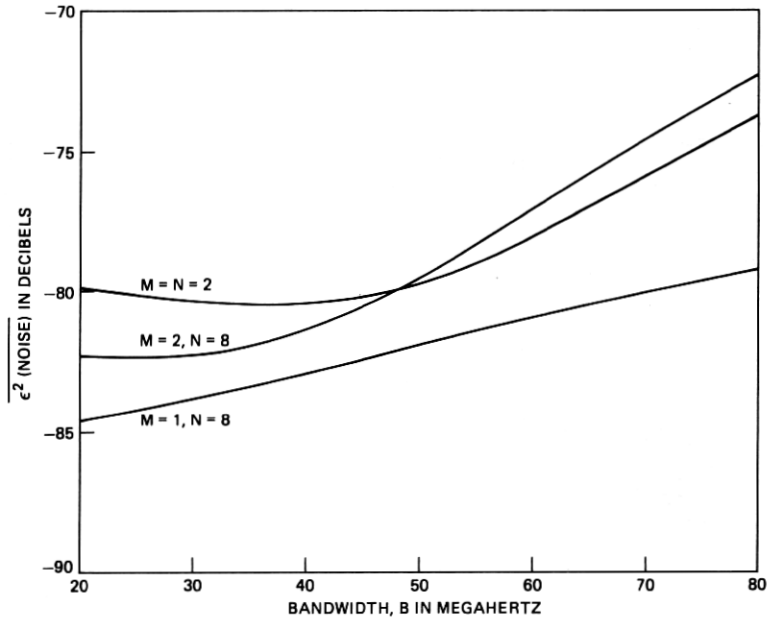

Fig. 2—Mean-square noise errors, $\overline{\epsilon^2(\text{noise})}$ in dB, for Cases 2 and 3 ($M = 2$, $N = 8$ and $M = 1$, $N = 8$). Results shown are for uniform tone powers; results for optimal tone powers are lower by less than 0.5 dB.

sometimes smaller when $N = 2$ and sometimes smaller when $N = 8$. The explanation lies in two offsetting factors: Using nine tones leads to less power per tone, but affords averaging benefits not available when using three tones. Depending on B, one or the other of these factors dominates.

(iii) For all three low-order polynomial approaches considered, $\overline{\epsilon^2(\text{noise})}$ is less than 10^{-7} for bandwidths up to 90 MHz or more.

4.4 Generalizations and extensions

We emphasize that $\overline{\epsilon^2(\text{noise})}$ in (37) scales readily in the quantities $bN_F/\bar{P}g_0^2$ and $B/\Delta f$. Therefore, the curves of Figs. 1 and 2, however particularized to the present experiment parameters, can easily be scaled to reflect other conditions.

With this in mind, we can account in a simple and fairly accurate way for both quantization noise (previously neglected) and changes in $\bar{P}$, g_0, b, and N_F. We assume the quantization and Gaussian noise powers to be additive, invoke (16) and (17), and obtain the following rule: If $bN_F/\bar{P}g_0^2$ is changed by a factor C from the one obtained using Table I, then $\overline{\epsilon^2(\text{noise})}$ should be adjusted by the factor $(C + 0.25)$. For $C = 1$ (no change in $bN_F/\bar{P}g_0^2$), quantizing noise adds roughly 25 percent (1 dB) to the mean-square noise error.

V. APPROXIMATION ERRORS

5.1 Method of analysis

The approximation error defined in (32) results from sampling $H(\omega)$ at a finite number of discretely-spaced frequencies. The mean-square error, as defined in (33), depends on B, Δf, M, N, and—unlike the noise error—on the specific function being approximated. We consider a highly accurate polynomial approximation to be one for which η, defined by

$$\eta \triangleq \overline{\epsilon^2(\text{approx})}/\overline{H^2}, \tag{42}$$

is less than or equal to 10^{-3}. Our aim here is to calculate η using a function for $H(\omega)$ that is "representative," in a sense to be described shortly. The method of computation, given $H(\omega)$, follows directly from the relationships in Section III.

The basic form assumed for $H(\omega)$ is the one used by W. D. Rummler in previous studies.[5,6,9] To fit measured amplitude responses in a 25.3-MHz bandwidth near 6 GHz, Rummler expressed $H(\omega)$ by the function $a[1 - b \exp(j\theta) \exp(-j\omega\Delta\tau)]$, where a, b, θ, and $\Delta\tau$ are function parameters to be chosen. For each of 24,920 response measurements, these four parameters were chosen to give a least-squares functional fit to the data. Error analyses of the results (Fig. 17 of Ref. 5) revealed a high degree of fitting accuracy over nearly all of the data records. For this reason, we use the same function here to represent the actual underlying response of multipath fading.

Rummler also analyzed the effect of fixing the delay parameter $\Delta\tau$ at 6.31 ns, and choosing (a, b, θ) to fit each data record. While not as good in all cases, the "fixed delay" model was found to be highly accurate over at least 98 percent of the data base. With this in mind, we conjecture that the above function, with $\Delta\tau \leq 10$ ns, can be used to represent the vast majority of MPF responses. We will invoke this conjecture later in tabulating bandwidths over which polynomials of specified order can be used to model multipath fading.

Our approach in what follows will be to find η for specified B and $\Delta\tau$, with b and θ chosen to give worst-case polynomial fitting results. This should provide conservative estimates of the limitations of polynomial fitting. We will also assume a phase adjustment to the function used by Rummler, to enforce consistency with the data processing approach described earlier. In particular, we specify the response function to be

$$H(\omega) = a(1 - be^{j\theta}e^{-j\omega\Delta\tau}) \exp[j(\Delta\Phi + \omega\Delta T)], \tag{43}$$

where $\Delta\Phi$ and ΔT were defined in Section II. As noted there, the data reduction process chooses $\Delta\Phi$ in such a way that $H(0)$ is made real, and chooses ΔT in such a way that η is minimized for a given Mth-

order polynomial fit. Accordingly, we specify that $\exp(j\Delta\Phi) = (1 - be^{-j\theta})/\sqrt{1 + b^2 - 2b\cos\theta}$; search over ΔT so as to minimize η for a given fitting polynomial and given (b, θ); and search over b and θ so as to maximize that minimized η.* Thus, we obtain the measure

$$\eta_0 \triangleq \underset{(b,\theta)}{\text{Max}} \left\{ \underset{\Delta T}{\text{Min}}(\eta) \right\}, \qquad \text{worst-case } \eta, \text{ given } \Delta\tau \text{ and } B. \tag{44}$$

We have done this for each of the different combinations of M and N described earlier, using $B\Delta\tau$ as a variable and B as a parameter. We now present our findings.

5.2 Results for Case 1 ($M = N = 2, 4, 6,$ or 8)

The worst-case combination of (b, θ) for any B, $\Delta\tau$, and polynomial order is found to be (1.0, 0.0). This combination corresponds to total fading at the band center ($\omega = 0$). Also, the optimal ΔT for $b = 1.0$ is precisely $\Delta\tau/2$.

The variations of η_0 with $B\Delta\tau$, with M and B as parameters, are shown in Fig. 3. As expected, η_0 is a strongly decreasing function of M, a strongly increasing function of $B\Delta\tau$, and a weakly increasing function of B alone for given $B\Delta\tau$.

A useful empirical formula for these results, accurate to within 40 percent for $B \leq 80$ MHz and $B\Delta\tau \leq 1.2$, is

$$\eta_0 = k(M, B)10^{-M}(B\Delta\tau)^{2M}[1 + \alpha(B\Delta\tau)], \tag{45}$$

where $\alpha = 0.57$ and $k(M, B)$ is a fairly mild function of M and B. Numerical values for $k(M, B)$ are given in Table IV.

5.3 Cases 2 and 3 ($M = 2$, $N = 8$ and $M = 1$, $N = 8$)

Curves of η_0 for these cases are shown in Fig. 4, where the results for $M = N = 2$ are repeated for comparison purposes. There is an evident improvement when second-order polynomials are derived using nine tones instead of three. An empirical formula for these results (again, accurate to within 40 percent for $B \leq 80$ MHz and $B\Delta\tau \leq 1.2$) is given by (45), where $\alpha = 0.32$; the power of $(B\Delta\tau)$ is replaced by 4; and numerical values for $k(M, B)$ are given in Table IV.

5.4 Optimizing ΔT using measured data

In minimizing η with respect to ΔT, (44), we used computer search procedures and exploited our assumed knowledge of the underlying $H(\omega)$. In an actual measurement the latter is not possible, as the only information available for optimizing ΔT is the set of measured G samples.

---

* The amplitude factor a has no impact on fitting accuracy and so is set to unity for purposes of this study.

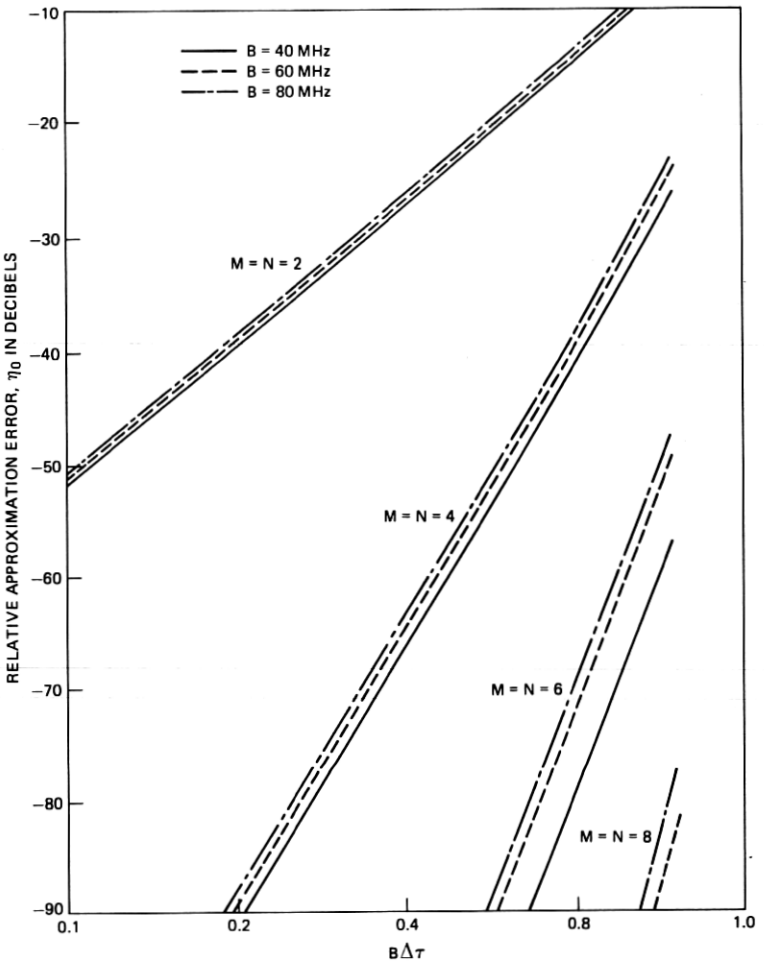

Fig. 3—Relative mean-square approximation errors, η_0 in dB, for Case 1 ($M = N = 2$, 4, 6, or 8). The variable is $B\Delta\tau$, where $\Delta\tau$ is the delay spread quantity in Eq. (43). Bandwidth, B, and M are parameters.

By experimenting with different strategies, we have identified a computationally efficient procedure that uses these samples to optimize ΔT. It consists of computing $C_2 \triangleq (A_2^2 + B_2^2)$ as a function of ΔT and choosing that ΔT for which C_2 is a minimum. The procedure is even simpler than it might seem; for, if $A_{n,o}$ is A_n computed for $\Delta T = 0$, then A_2 for any other ΔT is just

$$A_2 = A_{2,o} + A_{1,o}\Delta T + \tfrac{1}{2}A_{0,o}\Delta T^2, \tag{46}$$

and an identical relationship applies to B_2. These results can be

Table IV—Values of $k(M, B)$ in eq. (45)

Case	Case 1 ($M = N$)				Cases 2 and 3 ($N = 8$)	
$B \backslash M$	8	6	4	2	2	1
40 MHz	1.31×10^{-4}	0.138	3.32	6.39	1.47	1.51
60 MHz	1.95×10^{-2}	0.734	5.31	6.98	2.56	1.78
80 MHz	5.83×10^{-2}	1.14	6.17	7.20	4.26	2.26

derived using (6), (21), and (22), and the power series expansion of $\exp(j\omega\Delta T)$.

Thus, "optimizing" ΔT amounts to finding the minimum of a fourth-order polynomial in that quantity. This can be done very efficiently

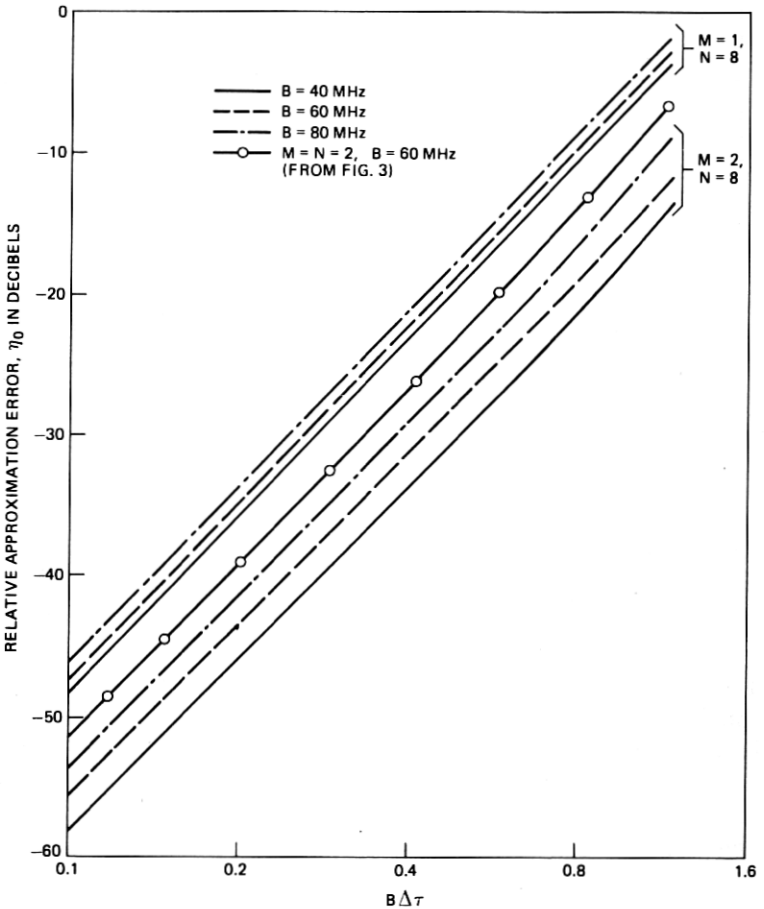

Fig. 4—Relative mean-square approximation error, η_0 in dB, for Cases 2 and 3 ($M = 2$, $N = 8$ and $M = 1$, $N = 8$). Same variable and parameters as in Fig. 3.

using computer algorithms. Our investigation of this procedure consisted of minimizing C_2 with respect to ΔT for numerous $(b, \theta, \Delta\tau)$, and using the resulting values of ΔT to compute η. We obtained remarkably similar answers, in most cases, to those obtained with ΔT rigorously optimized [i.e., via computer search using the known function $H(\omega)$]. The worst departures occur when η is either so large as to be of no interest or so small that the error increases do not matter.

Other measures derivable from the data, such as $[(A_2 - A_1^2)^2 + (B_2 - B_1^2)^2]$, may be even more appropriate Quantities such as this, or C_2 as defined above, are reliable indicators of the "curvature" in $H(\omega)$; choosing Δt to minimize them should therefore maximize the fitting accuracy of low-order polynomials. Our results give empirical support for this principle.

VI. SUMMARY AND CONCLUSION

The major findings of this study are summarized in Table V. The first row gives, for each combination of M and N considered, the bandwidth below which polynomial fitting yields $\overline{\epsilon^2(\text{noise})} \leq 10^{-7}$. These bandwidths are derived for uniform tone powers and the parameter values listed in Table I. They cannot be increased much without dramatic (and unlikely) improvements in transmitter power, noise bandwidths, and quantizing precision.

The second row of Table V gives the corresponding bandwidths below which $\eta \leq 10^{-3}$. They are derived for the response function (43), with b and θ having worst-case values and $\Delta\tau = 10$ ns. The third row gives the maximum bandwidth which satisfy *both* mean-square error requirements. Since these requirements are quite stringent, we present in the fourth row the results of relaxing both of them by 6 dB (factor of four).

These tabulations suggest that the vast majority of MPF responses can be accurately approximated, over bandwidths of 40 (62) MHz, by

Table V—Bandwidths, in MHz, over which $H(\omega)$ can be accurately characterized

Case	Case 1 ($M = N$)				Cases 2 and 3 ($N = 8$)	
Requirement \ M	8	6	4	2	2	1
$\overline{\epsilon^2(\text{noise})} \leq 10^{-7}$	40	34	55	96	90	180
$\eta \leq 10^{-3}$	140	125	96	35	48	28
Both requirements	40	34	55	35	48	28
Requirements relaxed 6 dB	43	37	62	48	62	40

Notes:
(1) Results assume $\Delta\tau = 10$ ns.
(2) Results in excess of 80 MHz are extrapolated estimates.

complex polynomial functions of just first (second) order. We surmise, then, that the appropriate modeling approach is to form first- and second-order polynomials using nine-tone measurements ($N = 8$) and least-squares data fitting. With these low orders, there is maximal simplicity in developing and using the model, with no substantial sacrifice in accuracy. By using nine tones, moreover, polynomials of higher order (up to eight) can also be deduced from the data, thereby enabling the theoretical predictions given here to be fully tested.

VII. ACKNOWLEDGMENT

We are grateful for the helpful comments of W. D. Rummler.

REFERENCES

1. W. C. Jakes, Jr., "An Approximate Method to Estimate an Upper Bound on the Effect of Multipath Delay Distortion on Digital Transmission," IEEE Trans. Commun., *COM-27,* No. 1 (January 1979).
2. L. J. Greenstein and V. K. Prabhu, "Analysis of Multipath Outage with Applications in 90-Mb/s PSK Systems at 6 and 11 GHz," IEEE Trans. Commun., *COM-27,* No. 1 (January 1979).
3. C. W. Anderson, S. Barber, and R. Patel, "The Effect of Selective Facing on Digital Radio," Int. Conf. Commun. 1978, Conf. Record, *2* (1978), pp. 33.5.1–6.
4. C. W. Lundgren and W. D. Rummler, "Digital Radio Outage Due to Selective Fading-Observation vs. Prediction from Laboratory Simulation," B.S.T.J., *58,* No. 7 (May–June 1979), pp. 1073–100.
5. W. D. Rummler, "A New Selective Fading Model: Application to Propagation Data," B.S.T.J., *58,* No. 7 (May–June 1979), pp. 1037–71.
6. W. D. Rummler, "Extensions of the Multipath Fading Channel Model," Int. Conf. Commun. 1979, Conf. Record, *2* (1979), pp. 32.2.1–5.
7. L. J. Greenstein and B. A. Czekaj, "A Statistical Model for Multipath Fading Channel Responses," Int. Conf. Commun. 1979, Conf. Record, *2* (1979), pp. 32.1.1–5.
8. L. J. Greenstein and B. A. Czekaj, "A Polynomial Model for Multipath Fading Channel Responses," B.S.T.J., *59,* No. 7 (September 1980), pp. 1197–225.
9. W. D. Rummler, "Advances in Multipath Channel Modeling," Int. Conf. Commun. 1980, Conf. Record, *3* (1980), pp. 52.3.1–5.
10. A. B. Crawford and W. C. Jakes, Jr., "Selective Fading of Microwaves," B.S.T.J., *31,* No. 1 (January 1952), pp. 68–90.
11. L. J. Greenstein and P. J. Fitzgerald, "Phasing Multitone Signals to Minimize Peak Factors," (to be published).
12. L. J. Greenstein, "A Multipath Fading Channel Model for Terrestrial Digital Radio Systems," IEEE Trans. Commun., *COM-26,* No. 8 (August 1978), pp. 1247–50.
13. J. R. Green and D. Margerison, *Statistical Treatment of Experimental Data,* New York: Elsevier, 1977, Chapter 15.